Direct binding between BubR1 and B56–PP2A phosphatase complexes regulate mitotic progression

Thomas Kruse, Gang Zhang*, Marie Sofie Yoo Larsen*, Tiziana Lischetti*, Werner Streicher*, Tine Kragh Nielsen, Sara Petersen Bjørn and Jakob Nilsson‡

The Novo Nordisk Foundation Center for Protein Research, Faculty of Health and Medical Sciences, University of Copenhagen, Blegdamsvej 3b, 2200 Copenhagen, Denmark

*These authors contributed equally to this work
‡Author for correspondence (jakob.nilsson@cpr.ku.dk)

Accepted 11 December 2012
Journal of Cell Science 126, 1086–1092

doi: 10.1242/jcs.122481

Summary

BubR1 is a central component of the spindle assembly checkpoint that inhibits progression into anaphase in response to improper kinetochore–microtubule interactions. In addition, BubR1 also helps stabilize kinetochore–microtubule interactions by counteracting the Aurora B kinase but the mechanism behind this is not clear. Here we show that BubR1 directly binds to the B56 family of protein phosphatase 2A (PP2A) regulatory subunits through a conserved motif that is phosphorylated by cyclin-dependent kinase 1 (Cdk1) and polo-like kinase 1 (Plk1). Two highly conserved hydrophobic residues surrounding the serine 670 Cdk1 phosphorylation site are required for B56 binding. Mutation of these residues prevents the establishment of a proper metaphase plate and delays cells in mitosis. Furthermore, we show that phosphorylation of serines 670 and 676 stimulates the binding of B56 to BubR1 and that BubR1 targets a pool of B56 to kinetochores. Our data suggest that BubR1 counteracts Aurora B kinase activity at improperly attached kinetochores by recruiting B56–PP2A phosphatase complexes.

Key words: BubR1, B56–PP2A, Kinetochore, Chromosome segregation

Introduction

Accurate segregation of sister chromatids during mitosis depends on their bi-orientation on the mitotic spindle such that the sister chromatids segregate to opposite poles at anaphase. Bi-orientation requires the establishment of proper connections between dynamic microtubules and kinetochores on sister chromatids (Santaguida and Musacchio, 2009; Welburn and Cheeseman, 2008). Kinetochores are able to stably bind to the dynamic plus ends of microtubules and in response to improper binding they activate the spindle assembly checkpoint (SAC) a conserved signaling pathway that delays the onset of anaphase (Musacchio and Salmon, 2007). In addition to their role in the SAC a subset of checkpoint proteins namely the kinases Aurora B, Mps1, Bub1 and BubR1 are required for proper kinetochore–microtubule interactions (Ditchfield et al., 2003; Hewitt et al., 2010; Klebig et al., 2009; Lampson and Kapoor, 2005; Maciejowski et al., 2010; Meraldi and Sorger, 2005; Santaguida et al., 2010; Welburn et al., 2010). Aurora B plays an important role in this process in that it phosphorylates a number of outer kinetochore proteins to destabilize the interaction with microtubules thus 'resetting' the kinetochore allowing new proper connections to form (Cheeseman et al., 2006; DeLuca et al., 2006; Welburn et al., 2010). How phosphorylations on outer kinetochore proteins are removed is not clear but both the PP1 and PP2A phosphatases have been implicated. Recently it was shown that PP2A in complex with regulatory subunits of the B56 family (also known as PPP2R5 or B′ subunits) localizes to kinetochores/centromeres of unattached chromosomes and dephosphorylates kinetochore proteins to establish proper kinetochore–microtubule interactions (Foley et al., 2011). However, it is not clear how B56–PP2A gets recruited to the kinetochore.

BubR1 binds to unattached kinetochores and counteracts Aurora B kinetochore phosphorylation by an unknown mechanism (Ditchfield et al., 2003; Lampson and Kapoor, 2005). The central region of BubR1 does not contain any obvious structural motifs but is required for the role of the protein in stabilizing kinetochore–microtubule interactions (Suijkerbuijk et al., 2010). This region of BubR1 is heavily phosphorylated by Cdk1 and Plk1 and the respective phosphorylation of S670 and S676 by these kinases is important for the role of BubR1 in stabilizing kinetochore–microtubule interactions (Elowe et al., 2010; Elowe et al., 2007; Huang et al., 2008).

Here we show that BubR1 binds directly to B56 regulatory subunits of the PP2A phosphatase through a short highly conserved region centered on the S670 phosphorylation site. BubR1 recruits a pool of B56 to the outer kinetochore and preventing their interaction interferes with chromosome segregation. We propose that in response to improperly attached kinetochores Cdk1 and Plk1 stimulates the recruitment of B56–PP2A complexes to the outer kinetochore through BubR1 and, in turn, this counteracts Aurora B kinase activity.

Results and Discussion

BubR1 binds to PP2A regulatory subunits during mitosis

To understand how BubR1 functions during mitosis we used a yeast two-hybrid approach to screen a human placenta cDNA library using full length BubR1 as bait. The most prominent interactors identified were the five members of the B56 family of

protein phosphatase PP2A regulatory subunits (Fig. 1A). To determine whether BubR1 interacts with the B56–PP2A complex *in vivo* we immunopurified endogenous BubR1 from cells arrested in mitosis with nocodazole or from asynchronous growing cells. Although we have not been able to detect any members of the B56 family in BubR1 purifications we consistently enriched the catalytic subunit of PP2A in the mitotic sample (Fig. 1B). Given the evidence presented later we believe that the interaction between BubR1 and PP2AC is mediated by the B56 subunits.

To further validate the interaction we generated a HeLa cell line stably expressing Venus-tagged B56α. The Venus B56α fusion appeared functional in that it co-purified two proteins at almost stoichiometric levels corresponding in size to the PP2A catalytic and PP2A scaffold proteins and localized to kinetochores/centromeres in mitosis (supplementary material Fig. S1A,B). We purified Venus B56α and analyzed its ability to co-purify BubR1 from mitotic or interphase cells. In mitosis we observed a robust binding to BubR1 that was reduced in the interphase sample while binding to the catalytic subunit was constant (Fig. 1C). We also tested binding to Venus tagged B56β and B56γ and compared this to the unrelated B55α subunit. Again we observed efficient co-purification of BubR1 from the mitotic sample and this was more efficient with the B56 subunits than the B55 subunit (supplementary material Fig. S1C).

Combined these results show that BubR1 interacts with the B56–PP2A complex and that this interaction is stronger during mitosis.

A)

Protein	# clones	Confidence score
B56α	6	Very high
B56β	6	Very high
B56γ	6	Very high
B56δ	5	Very high
B56ε	8	Low
HOPX	9	Very high
DHX8	3	High
Cdc20	1	Moderate

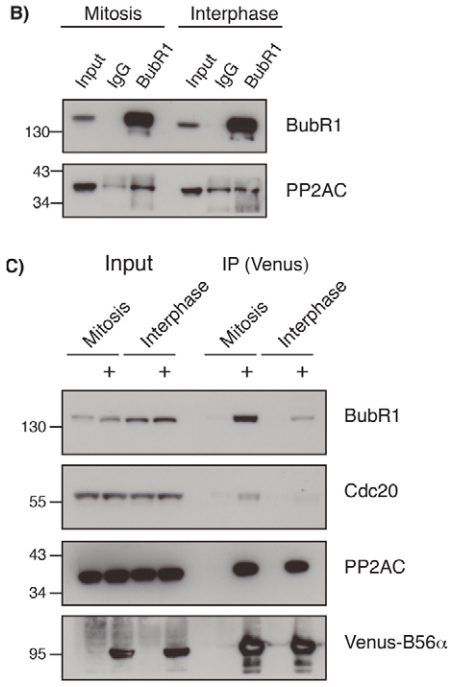

Fig. 1. BubR1 interacts with the B56–PP2A complex during mitosis. (**A**) Protein interaction with human BubR1 in a yeast two-hybrid screen using full-length BubR1 as a bait and a human placenta cDNA library as prey. The interacting proteins were assigned a confidence score. (**B**) Endogenous BubR1 was immunopurified from HeLa cells arrested in mitosis with nocodazole or from asynchronously growing cells and analyzed for the presence of PP2AC and compared with control purification. Input was the same for both the IgG and BubR1. (**C**) Venus B56α was expressed (indicated by +) in a stable inducible cell line and then purified and the association of BubR1, Cdc20 and PP2AC analyzed by western blot. Venus B56α was either purified from cells arrested with nocodazole or from asynchronous growing cells.

B56 subunits bind to a conserved region in BubR1 that is phosphorylated by Plk1 and Cdk1

To determine how B56 subunits interact with BubR1 we made 5 constructs of BubR1 covering different functional domains and analyzed the ability of these to interact with B56α in the yeast two-hybrid system. We detected binding to all fragments containing the region 555–700 (supplementary material Fig. S2A). This region of BubR1 has been reported to be involved in the alignment of chromosomes and formation of stable kinetochore–microtubule interactions and indeed we could confirm this by comparing mitotic progression in RNAi rescue experiments with BubR1 1–483 and BubR1 1–715 (supplementary material Fig. S2B).

To determine if this binding was direct we purified a recombinant fragment of BubR1 encompassing amino acids 516–715 (BubR1 555–700 did not express) and tested whether this could bind recombinant B56α. The two proteins were run individually on a Superdex 200 size exclusion column and fractions analyzed by SDS-PAGE (Fig. 2B). B56α migrated at the expected size while BubR1 516–715 migrated around 90 kDa indicating that this BubR1 fragment is either a multimer or elongated. When the two proteins were mixed prior to loading on the column they co-eluted from the column as a complex of ~150 kDa showing that B56α can bind directly to BubR1 516–715.

To identify the residues in BubR1 binding to B56α we made a 20mer peptide array covering the residues 555–700 of BubR1 with a three amino acid shift between peptides. Two arrays were treated identically except one was incubated with recombinant B56α protein and then both arrays were incubated with a B56α specific antibody. Three peptides bound strongly to B56α and they covered the region 660–685 (Fig. 2C). To further identify the binding site we generated a second peptide array using a template peptide covering amino acids 663–682 and then performed an alanine scan through the sequence. Incubation with B56α revealed that B56α binding was abolished when L669 or I672 where mutated to alanine while K668 and E674 also contributed to the interaction (Fig. 2D). The identified residues required for B56α to bind BubR1 are strictly conserved and surround the conserved S670 Cdk1 phosphorylation site (Fig. 2E) (Elowe et al., 2010; Huang et al., 2008). To determine if the same residues were required *in vivo* for binding to B56α we transfected the Venus B56α cell line with mCherry tagged BubR1 WT, BubR1 Δ660–685 and BubR1 L669A/I672A and purified Venus B56α from mitotic cells. While the endogenous BubR1 was equally enriched in the different samples only mCherry BubR1

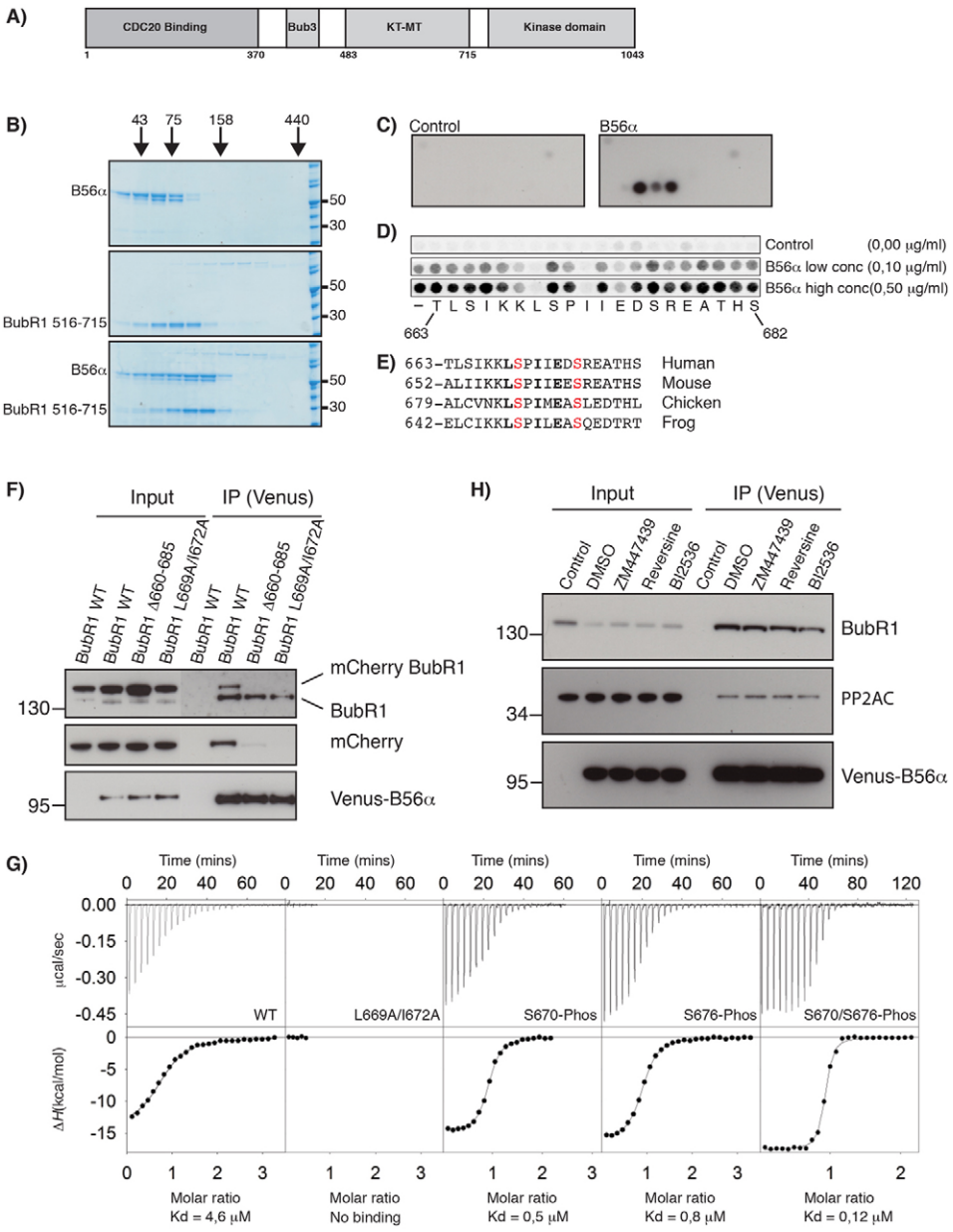

Fig. 2. B56 subunits bind to a conserved region in BubR1. (**A**) Schematic of BubR1 primary structure with functional domains indicated. (**B**) Recombinant B56α and BubR1 516–715 were run on a Superdex 200 column and samples analyzed. The migration of globular proteins with the indicated molecular weight on the column is indicated on top. The top gel is the migration of B56α alone, the middle gel the migration of BubR1 516–715 alone and the lowest gel the migration of B56α and BubR1 516–715 incubated before running on the column. (**C**) 20mer peptide arrays covering amino acids 555–700 of BubR1 either incubated with recombinant B56α or untreated and then stained with a B56α antibody and developed. (**D**) Peptide array using a peptide corresponding to BubR1 663–682. Then alanine was introduced at each position and the samples treated as in C using two different concentrations of B56α. (**E**) Alignment of 663–682 BubR1 sequences from human, mouse, chicken and frog, with the residues required for B56 binding indicated in bold and the S670 and S676 phosphorylation sites indicated in red. (**F**) A cell line expressing Venus B56α was transfected with the indicated mCherry BubR1 constructs and Venus B56α purified. The association of endogenous and exogenous BubR1 was then analyzed. The gel is combined from two different exposures. (**G**) ITC measurements of the binding of B56α to the BubR1 660–682 peptide and binding to the same peptide with either L669A/I672A or S670 and S676 phosphorylated individually or combined. Stoichiometry was 0.85–0.9 for all peptides. (**H**) Venus B56α was purified from nocodazole and MG132 arrested cells incubated with the indicated kinase inhibitors for 2 hours and the association with BubR1 and PP2AC analyzed by western blot.

WT bound to Venus B56α confirming that indeed the residues identified by the peptide array experiments are critical for binding *in vivo* (Fig. 2F).

To further characterize the interaction we used isothermal titration calorimetry (ITC) and measured the affinity of purified B56α for a BubR1 peptide encompassing amino acids 660–682. This peptide bound to B56α with a K_d of 4.6 μM whereas when L669 and I672 were mutated to alanine the binding was completely abolished (Fig. 2G). To determine if phosphorylations on S670 and S676 affected the binding to B56α we measured the affinity of the same peptide with phosphorylations on either S670 or S676 or both sites phosphorylated. When S670 was phosphorylated the peptide bound to B56α with a K_d of 0.5 μM while phosphorylation of S676 lowered the K_d to 0.8 μM and the double phosphorylated peptide bound with a K_d of 0.12 μM. This reveals that phosphorylation of S670 or S676 stimulates the interaction between B56α and the BubR1 peptide *in vitro*, which is in line with our observation that BubR1 and B56 subunits interacted stronger during mitosis. Indeed when we inhibited Plk1 in mitotic cells there was a slight reduction in the interaction between BubR1 and B56 (Fig. 2H).

Our results show that B56 subunits bind directly to a conserved region in BubR1 centered on the Cdk1 S670 phosphorylation site and that the conserved L669 and I672 are required for B56 binding. The binding of B56 subunits to BubR1 is stimulated by phosphorylation of S670 and S676 revealing that Cdk1 and Plk1 can stimulate the binding. Since phosphorylation of BubR1 on S670 and S676 appears to happen exclusively at unattached and tension-less kinetochores respectively (Elowe et al., 2010; Huang et al., 2008) our results suggest that the binding between BubR1 and B56 is stimulated in response to improper kinetochore microtubule attachments and that the two proteins interact at the kinetochore.

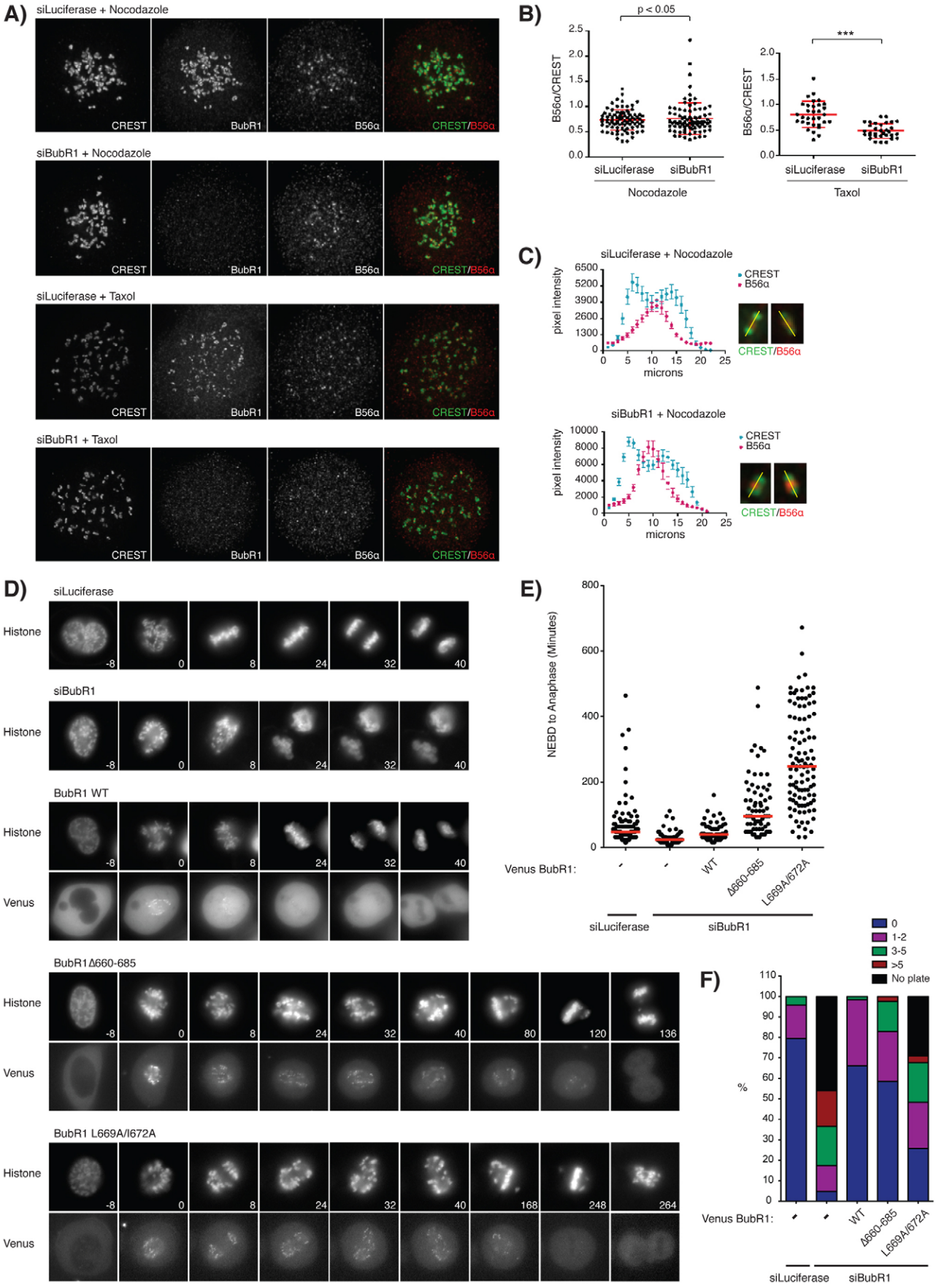

Fig. 3. See next page for legend.

Binding of BubR1 to B56 subunits is required for proper chromosome segregation

To determine if BubR1 regulates the recently described localization of B56 subunits to the kinetochore (Foley et al., 2011) we analyzed B56α localization in taxol or nocodazole arrested cells depleted of BubR1 and compared it to control treated cells. In taxol treated cells we observed an approximate 50% reduction in total B56α levels at the kinetochore/centromere when BubR1 was depleted while in nocodazole arrested cells the total levels appeared similar (Fig. 3A,B). However when we inspected the line profile of B56α staining through the kinetochore/centromere of sister chromatids in nocodazole arrested cells it was clear that BubR1 depletion resulted in a sharper profile (Fig. 3C). This shows that BubR1 can recruit a subset of B56 to the outer kinetochore in both taxol and nocodazole arrested cells.

To determine if the interaction between BubR1 and B56–PP2A complexes is critical for chromosome segregation we analyzed the ability of fluorescent RNAi resistant BubR1 WT, BubR1 Δ660–685 and BubR1 L669A/I672A to rescue the chromosome alignment defect observed when endogenous BubR1 was depleted. In the absence of BubR1 cells rapidly progressed through mitosis and no clear metaphase plate was visible (Fig. 3D–F) whereas the introduction of BubR1 WT restored mitotic timing and chromosome alignment. Cells complemented with BubR1 Δ660–685 and BubR1 L669A/I672A arrested in mitosis for a prolonged time with several unaligned chromosomes indicating that BubR1 binding to B56–PP2A complexes is critical for chromosome alignment (Fig. 3D–F).

Using a similar approach we also analyzed the phenotype by immunofluorescence under the different rescue conditions (Fig. 4A–C). We treated cells for 2 hours with MG132 to maintain them in mitosis and then either fixed them directly or kept them on ice for 15 minutes before fixation to depolymerize non-kinetochore microtubules. Similar to what we observed by time-lapse microscopy, cells expressing BubR1 WT formed a metaphase plate while BubR1 Δ660–685 and BubR1 L669A/I672A expressing cells had numerous unaligned chromosomes that lacked cold stable microtubules (Fig. 4A–C).

Here we have revealed a novel interaction between BubR1 and the B56–PP2A complex that is critical for chromosome segregation and our work provides insight into how Cdk1 and Plk1 help establish stable kinetochore–microtubule interactions in prometaphase by stabilizing the interaction between BubR1 and B56 subunits to counteract Aurora B. Interestingly the individual phosphorylations on S670 and S676 of BubR1 both stabilize the binding to B56 and combined they further increase the affinity indicating that the levels of B56–PP2A complexes on kinetochores could be fine tuned by combinations of these phosphorylations depending on the microtubule binding state of the kinetochore. While this work was being prepared for submission a study from the Kops lab came to similar conclusions and they identify T680 as a novel Plk1 site that also stimulates the interaction between BubR1 and B56 (Suijkerbuijk et al., 2012). Understanding how these phosphorylations increases the binding between BubR1 and B56 and how Plk1 and Cdk1 monitors microtubule-kinetochore interactions will be an important topic for future research.

Fig. 3. Interaction between BubR1 and B56 is required for proper chromosome segregation. (**A**) Localization of B56α and BubR1 in control (luciferase RNAi-treated) or BubR1 RNAi-treated cells arrested with nocodazole or taxol. (**B**) Quantification of B56α on individual kinetochores and normalization to CREST levels, with the median indicated by the line. For the nocodazole condition, the number of kinetochore pairs analyzed was 85 and for the taxol condition 35 kinetochore pairs were analyzed (**C**) Line-profile of B56α (red) and CREST (blue) staining through individual sister chromatid pairs in nocodazole-arrested cells. The average curves of 14 kinetochore pairs for the control and 19 for the BubR1 depleted cells are shown. (**D**) Representative time-lapse images from the indicated conditions, with time at nuclear envelope breakdown (NEBD) set to zero. (**E**) Plot of NEDB-to-anaphase times in the indicated conditions. At least 70 cells were analyzed per condition (**F**) Quantification of number of unaligned chromosomes in the last frame before cells enter anaphase in the indicated conditions. Three z-stacks with a spacing of 5 μm were inspected and at least 30 cells were analyzed for each condition. ***$P<0.0001$.

Materials and Methods

Two-hybrid analysis

Yeast two-hybrid screening was performed by Hybrigenics Services, S.A.S.

The full length coding sequence for BubR1 (GenBank accession number gi: 168229167) was PCR-amplified and cloned into pB29 as an N-terminal fusion to LexA (N-BubR1-LexA-C). The construct was checked by sequencing the entire insert and used as a bait to screen a random-primed Human Placenta cDNA library constructed into pP6. 68.1 million clones (6.8-fold the complexity of the library) were screened using a mating approach with Y187 (matα) and L40ΔGal4 (mata) yeast strains. 172 His+ colonies were selected on a medium lacking tryptophan, leucine and histidine, and supplemented with 10 mM 3-aminotriazole to handle bait autoactivation. The prey fragments of the positive clones were amplified by PCR and sequenced at their 5′ and 3′ junctions. A confidence score was attributed to each interaction.

Antibodies

The following antibodies were used at the indicated dilutions for western blot. BubR1 (WB, A300-995A, 1:1000, Bethyl Laboratories), BubR1 (IF, A300-386A, 1:1000, Bethyl), BubR1 (monoclonal produced in-house used for IP), CDC20 (sc-13162, 1:1000, Santa Cruz), PP2A catalytic subunit (05-421, 1:2000, Millipore), GFP (ab290, 1:4000, abcam), B56α (610, 615, 1:3000, BD Biosciences), CREST (Antibodies Inc., 1:400)

Cloning

Full length B56α, B56β, B56γ and B55α were amplified from Invitrogen Ultimate clones by PCR and cloned into *Bam*HI and *Not*I sites of pcDNA5/FRT/TO 3*FLAG-Venus. BubR1 1–483 and 1–715 was obtained by amplifying the corresponding region of BubR1 from pcDNA5/FRT/TO 3*FLAG Venus BubR1 (siRES) (Bolanos-Garcia et al., 2011) and inserting into the *Bam*HI and *Not*I sites of pcDNA5/FRT/TO 3*FLAG Venus. BubR1 Δ660–685 was obtained by two step PCR using pcDNA5/FRT/TO 3*FLAG Venus BubR1 (siRES) as template and inserted into *Bam*HI and *Not*I sites of pcDNA5/FRT/TO 3*FLAG Venus. pcDNA5/FRT/TO 3*FLAG Venus BubR1 L669A/I672A was generated by whole plasmid PCR. BubR1, BubR1Δ660–685 and BubR1 L669A/I672A were subcloned into pcDNA3.1 mCherry vector using *Bam*HI and *Not*I sites. All constructs were verified by sequencing.

The *E. coli* expression plasmid 2A5A-c001 for expression of B56α was constructed by ligating a PCR amplified insert into vector pCPR0011 through ligation independent cloning. The PCR primers were 2A5A-2FW: tacttccaatccatgTCGTCGTCGTCG-CCGCCG and 2A5A-484RV: tatccacctttactgttaACTTGTATTGCTGAGAATA-CTGTGCATGTTGTAAG. pCPR0011 is a derivative of pNIC28-Bsa4 (GenBank Acc EF198106) where a StrepII tag (WSHPQFEK) has been inserted between the His-tag and the TEV-cleavage site.

The expression plasmid for BubR1 516–715 was constructed by ligating a PCR amplified insert into vector pCPR0005 through ligation independent cloning. (pCPR0005 is a derivative of pNIC28-Bsa4 (GenBank Acc EF198106) where a FLAG-HA tag (DYKDDDDK-YPYDVPDYA) has been inserted between the His-tag and the TEV-cleavage site. The PCR template was entry clone IOH21121 (Invitrogen) containing the BubR1 coding sequence and the PCR primers were BUB1B-1-516FW: tacttccaatccatgCAGGAACAACCTCATTCTAAAGGTCCC and BUB1B-1-715Rev: tatccacctttactgttaTTCTGAAGTCTCATTAGTAAGTTC-TAGTTTCTCAG.

Protein expression and purification

Proteins were expressed in the *E. coli* strain BL21 Rosetta2 (DE3) R3 T1 at 18˚for 20 hours using 0.5 mM IPTG. The pellets were resuspended in buffer L (50 mM NaP, 300 mM NaCl, 10% glycerol, 0.5 mM TCEP, pH 7.5) containing protease inhibitors and lyzed with a high-pressure homogeniser at 1000 Bar. The lysate was centrifuged at 18,500 ***g*** for 30 minutes and the supernatant filtered through a 0.22 μm PES filter and loaded onto a 1 ml Ni column (GE healthcare) in buffer L with 10 mM immidazole, washed and eluted. The eluate was loaded on a Superdex 200 PG 16/60 equilibrated with SEC buffer (50 mM NaP, 150 mM NaCl, 0.5 mM TCEP, 10% glycerol, pH 7.50) and fractions analyzed by SDS-PAGE. All proteins verified by mass spectrometry.

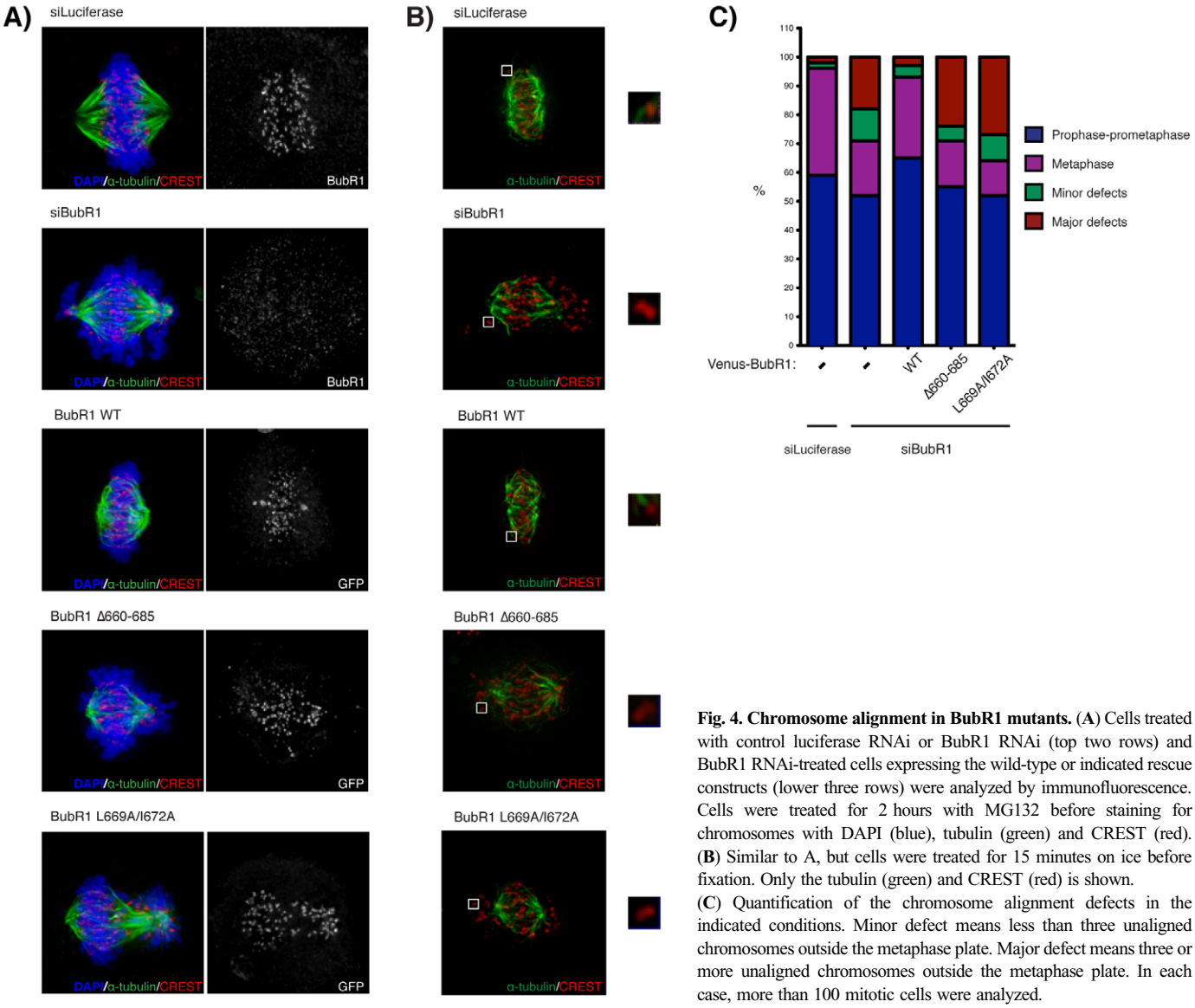

Fig. 4. Chromosome alignment in BubR1 mutants. (**A**) Cells treated with control luciferase RNAi or BubR1 RNAi (top two rows) and BubR1 RNAi-treated cells expressing the wild-type or indicated rescue constructs (lower three rows) were analyzed by immunofluorescence. Cells were treated for 2 hours with MG132 before staining for chromosomes with DAPI (blue), tubulin (green) and CREST (red). (**B**) Similar to A, but cells were treated for 15 minutes on ice before fixation. Only the tubulin (green) and CREST (red) is shown. (**C**) Quantification of the chromosome alignment defects in the indicated conditions. Minor defect means less than three unaligned chromosomes outside the metaphase plate. Major defect means three or more unaligned chromosomes outside the metaphase plate. In each case, more than 100 mitotic cells were analyzed.

Size exclusion chromatography

A Superdex 200 10/300 (GE healthcare) column was equilibrated with SEC buffer and 250 µg of B56α or BubR1 516–715 run on the column with a flow-rate of 0.4 ml/minute and 0.5 ml fractions collected. 250 µg B56α and 250 µg BubR1 516–715 were mixed in SEC buffer and incubated on ice for 1 hour before loading on the column.

Peptide array experiments

Peptide arrays were synthesized using a ResPepSL Bioanalytical Instrument (Intavis, Köln, Germany) on derivatized cellulose membranes using standard Fmoc [N-(9-fluorenyl)methoxycarbonyl] chemistry according to the manufacturer's instructions. For B56α binding experiments, purified recombinant B56α was added at the indicated concentrations in PBST (0.05% tween 20) containing 3% BSA and incubated together with the membrane overnight at 4℃. Membranes were washed three times in PBST and bound protein was visualized with anti-B56α antibodies and HRP or fluorescently conjugated antibodies.

ITC measurements

The following purified peptides were purchased from Biosyntan GmbH (Berlin, Germany): WT: YSQTLSIKKLSPIIEDSREATHS, L669A/I672A: YSQTLSI-KKASPAIEDSREATHS, S670(Phos): YSQTLSIKKL-pS-PIIEDSREATHS, S676(Phos): YSQTLSIKKLSPIIED-pS-REATHS and S670/S676(Phos): YSQT-LSIKKL-pS-PIIED-pS-REATHS. The peptides and B56α were extensively dialyzed into 50 mM sodium phosphate, 150 mM NaCl, 0.5 mM TCEP [*tris*(2-carboxyethyl)phosphine], 5% glycerol, pH 7.5. Protein and peptide concentrations were determined by UV spectroscopy and molar extinction coefficients at 280 nm of 1490 and 47,245 $M^{-1}cm^{-1}$ for the peptides and B56α, respectively. Isothermal Titration Calorimetry (ITC) experiments were performed at 25℃ using an ITC200 instrument (Microcal). 1.5 µl volumes of peptide, at ~450 µM, were titrated into the ITC sample cell containing ~35 µM of B56α, until saturation was achieved. Blank titrations of peptide into buffer were performed to determine peptide dilution heat effects and in all cases these were negligible. For the L669A/I672A peptide, no binding was observed at 25℃ and the experiment was repeated at 10℃ to take into account potential differences in binding ΔC_p (change in heat capacity) which could lead to no heat effects being observed at 25℃. The heat of the reaction was obtained by integrating each peak after the injection of peptide and fit to a model describing a single binding site using software provided by the ITC200 manufacturer.

Immunoprecipitation experiments

Cells were lysed in lysis buffer (50 mM Tris-HCl pH 7.5, 50 mM NaCl, 1 mM EDTA, 1 mM DDT and 0.1% NP40). Complexes were immunoprecipitated in lysis buffer with antibodies coupled to Protein G-Sepharose 4B (Invitrogen) or GFP-Trap (ChromoTek) beads as indicated and incubated at 4℃ for 2 hours or 30 minutes, respectively. Precipitated protein complexes were washed in washing buffer (50 mM Tris-HCl pH 7.5, 1 mg/ml BSA, 20% glycerol and 1 mM DTT) and eluted in 2×SDS sample buffer. The purification of Venus

tagged BubR1 constructs was performed as described previously (Bolanos-Garcia et al., 2011).

Tissue culture work

HeLa cells were maintained in DMEM with 10% serum. The following drug concentrations were used: Thymidine 2.5 μM, MG132 10 μM, Nocodazole 200 ng/μl, Taxol 200 ng/μl, Reversine 0.5 μM, ZM447439 2 μM, BI2536 0.5 μM.

Live cell analysis

Live cell analysis and immunofluorescence was performed as described previously (Bolanos-Garcia et al., 2011; Zhang et al., 2012) using a Deltavision Elite microscope (GE Healthcare). The BubR1 RNAi rescue experiments were done as described in Bolanos-Garcia et al. (Bolanos-Garcia et al., 2011) except that cells were transiently transfected with Venus-BubR1 constructs and CFP-Histone H3 together with 100 nM RNAi oligo targeting BubR1 using lipofectamine 2000 (Invitrogen). After 24 hours the cells were filmed using a 40×, 1.35 NA, WD 0.10 objective. All data analysis was performed using the softworx software (GE Healthcare).

Immunofluorescence

For immunofluorescence microscopy cells were synchronized with 2.5 mM thymidine, 10 μM MG132 and 200 ng/μl nocodazole. Cells were pre-fixed with 4% PFA in PHEM buffer (50 mM PIPES, 25 mM HEPES, 10 mM EGTA, 8.5 mM $MgSO_4$, pH 7.0) for 20 seconds, permeabilized in 0.5% Triton X-100 in PHEM buffer for 5 minutes and fixed in 4% PFA in PHEM buffer for 20 minutes. Coverslips were quenched with 25 mM Glycin in PBS for 20 minutes, blocked with 3% BSA in PBS-T (0.1% Tween in PBS) for 30 minutes, incubated with primary antibodies for 1 hour, with Alexa Fluor goat secondary antibodies for 45 minutes and mounted on slides using ProLong Gold Antifade mounting media (Invitrogen). Images were acquired taking z stacks of 200 nm using a 100×/1.4NA objective on a Deltavision Elite Microscope (Applied Precision). Images were analyzed after deconvolution using SoftWoRx (Applied Precision Instrument). Figures were generated by maximum intensity projection of entire cells using Softworx and ImageJ.

Acknowledgements

We thank Sabine Elowe for plasmids and Stephen Taylor for the HeLa/FRT/TRex cell line. We thank Geert Kops for communicating results before publication and Mikkel Staberg for help with peptide arrays and Mia Funk Nielsen for help with protein production. The authors have no conflict of interest.

Author contributions

T.K. performed the experiments shown in Figs 1 and 2, except that shown in Fig. 2B, which was performed by J.N. Experiments shown in Fig. 2G were performed by W.S., G.Z. performed the experiments shown in Fig. 4, M.S.Y.L those shown in experiments in Fig. 3D–F and T.L. performed the experiments shown in Fig 3A–C. T.K.N and S.P.B produced and purified recombinant proteins. J.N. designed the experiments together with the other authors and wrote the paper.

Funding

This work was supported by grants from the Novo Nordisk Foundation, the Lundbeck Foundation, and The Danish Council for Independent Research-FNU (all to J.N.); and a grant from The Danish Council for Independent Research-FSS to G.Z.

Supplementary material available online at
http://jcs.biologists.org/lookup/suppl/doi:10.1242/jcs.122481/-/DC1

References

Bolanos-Garcia, V. M., Lischetti, T., Matak-Vinković, D., Cota, E., Simpson, P. J., Chirgadze, D. Y., Spring, D. R., Robinson, C. V., Nilsson, J. and Blundell, T. L. (2011). Structure of a Blinkin-BUBR1 complex reveals an interaction crucial for kinetochore-mitotic checkpoint regulation via an unanticipated binding Site. *Structure* **19**, 1691-1700.

Cheeseman, I. M., Chappie, J. S., Wilson-Kubalek, E. M. and Desai, A. (2006). The conserved KMN network constitutes the core microtubule-binding site of the kinetochore. *Cell* **127**, 983-997.

DeLuca, J. G., Gall, W. E., Ciferri, C., Cimini, D., Musacchio, A. and Salmon, E. D. (2006). Kinetochore microtubule dynamics and attachment stability are regulated by Hec1. *Cell* **127**, 969-982.

Ditchfield, C., Johnson, V. L., Tighe, A., Ellston, R., Haworth, C., Johnson, T., Mortlock, A., Keen, N. and Taylor, S. S. (2003). Aurora B couples chromosome alignment with anaphase by targeting BubR1, Mad2, and Cenp-E to kinetochores. *J. Cell Biol.* **161**, 267-280.

Elowe, S., Hümmer, S., Uldschmid, A., Li, X. and Nigg, E. A. (2007). Tension-sensitive Plk1 phosphorylation on BubR1 regulates the stability of kinetochore microtubule interactions. *Genes Dev.* **21**, 2205-2219.

Elowe, S., Dulla, K., Uldschmid, A., Li, X., Dou, Z. and Nigg, E. A. (2010). Uncoupling of the spindle-checkpoint and chromosome-congression functions of BubR1. *J. Cell Sci.* **123**, 84-94.

Foley, E. A., Maldonado, M. and Kapoor, T. M. (2011). Formation of stable attachments between kinetochores and microtubules depends on the B56-PP2A phosphatase. *Nat. Cell Biol.* **13**, 1265-1271.

Hewitt, L., Tighe, A., Santaguida, S., White, A. M., Jones, C. D., Musacchio, A., Green, S. and Taylor, S. S. (2010). Sustained Mps1 activity is required in mitosis to recruit O-Mad2 to the Mad1-C-Mad2 core complex. *J. Cell Biol.* **190**, 25-34.

Huang, H., Hittle, J., Zappacosta, F., Annan, R. S., Hershko, A. and Yen, T. J. (2008). Phosphorylation sites in BubR1 that regulate kinetochore attachment, tension, and mitotic exit. *J. Cell Biol.* **183**, 667-680.

Klebig, C., Korinth, D. and Meraldi, P. (2009). Bub1 regulates chromosome segregation in a kinetochore-independent manner. *J. Cell Biol.* **185**, 841-858.

Lampson, M. A. and Kapoor, T. M. (2005). The human mitotic checkpoint protein BubR1 regulates chromosome-spindle attachments. *Nat. Cell Biol.* **7**, 93-98.

Maciejowski, J., George, K. A., Terret, M.-E., Zhang, C., Shokat, K. M. and Jallepalli, P. V. (2010). Mps1 directs the assembly of Cdc20 inhibitory complexes during interphase and mitosis to control M phase timing and spindle checkpoint signaling. *J. Cell Biol.* **190**, 89-100.

Meraldi, P. and Sorger, P. K. (2005). A dual role for Bub1 in the spindle checkpoint and chromosome congression. *EMBO J.* **24**, 1621-1633.

Musacchio, A. and Salmon, E. D. (2007). The spindle-assembly checkpoint in space and time. *Nat. Rev. Mol. Cell Biol.* **8**, 379-393.

Santaguida, S. and Musacchio, A. (2009). The life and miracles of kinetochores. *EMBO J.* **28**, 2511-2531.

Santaguida, S., Tighe, A., D'Alise, A. M., Taylor, S. S. and Musacchio, A. (2010). Dissecting the role of MPS1 in chromosome biorientation and the spindle checkpoint through the small molecule inhibitor reversine. *J. Cell Biol.* **190**, 73-87.

Suijkerbuijk, S. J. E., van Osch, M. H. J., Bos, F. L., Hanks, S., Rahman, N. and Kops, G. J. P. L. (2010). Molecular causes for BUBR1 dysfunction in the human cancer predisposition syndrome mosaic variegated aneuploidy. *Cancer Res.* **70**, 4891-4900.

Suijkerbuijk, S. J. E., Vleugel, M., Teixeira, A. and Kops, G. J. P. L. (2012). Integration of kinase and phosphatase activities by BUBR1 ensures formation of stable kinetochore-microtubule attachments. *Dev. Cell* **23**, 745-755.

Welburn, J. P. I. and Cheeseman, I. M. (2008). Toward a molecular structure of the eukaryotic kinetochore. *Dev. Cell* **15**, 645-655.

Welburn, J. P. I., Vleugel, M., Liu, D., Yates, J. R., 3rd, Lampson, M. A., Fukagawa, T. and Cheeseman, I. M. (2010). Aurora B phosphorylates spatially distinct targets to differentially regulate the kinetochore-microtubule interface. *Mol. Cell* **38**, 383-392.

Zhang, G., Kelstrup, C. D., Hu, X.-W., Hansen, M. J. K., Singleton, M. R., Olsen, J. V. and Nilsson, J. (2012). The Ndc80 internal loop is required for recruitment of the Ska complex to establish end-on microtubule attachment to kinetochores. *J. Cell Sci.* **125**, 3243-3253.